Published in "Antimicrobial Agents and Chemotherapy 60(5): 3032–3040, 2016"
which should be cited to refer to this work.

Intraspecies Transfer of the Chromosomal *Acinetobacter baumannii* bla_{NDM-1} Carbapenemase Gene

Thomas Krahn,[a] Daniel Wibberg,[a] Irena Maus,[a] Anika Winkler,[a] Séverine Bontron,[c] Alexander Sczyrba,[b] Patrice Nordmann,[c,d] Alfred Pühler,[a] Laurent Poirel,[c] Andreas Schlüter[a]

Institute for Genome Research and Systems Biology, Center for Biotechnology (CeBiTec), Bielefeld University, Bielefeld, Germany[a]; Computational Metagenomics, Faculty of Technology, Bielefeld University, Bielefeld, Germany[b]; Emerging Antibiotic Resistance Unit, Medical and Molecular Microbiology, Department of Medicine, Faculty of Science, University of Fribourg, Fribourg, Switzerland[c]; HFR - Hôpital Cantonal, Fribourg, Switzerland[d]

The species *Acinetobacter baumannii* is one of the most important multidrug-resistant human pathogens. To determine its virulence and antibiotic resistance determinants, the genome of the nosocomial bla_{NDM-1}-positive *A. baumannii* strain R2090 originating from Egypt was completely sequenced. Genome analysis revealed that strain R2090 is highly related to the community-acquired Australian *A. baumannii* strain D1279779. The two strains belong to sequence type 267 (ST267). Isolate R2090 harbored the chromosomally integrated transposon Tn*125* carrying the carbapenemase gene bla_{NDM-1} that is not present in the D1279779 genome. To test the transferability of the metallo-β-lactamase (MBL) gene region, the clinical isolate R2090 was mated with the susceptible *A. baumannii* recipient CIP 70.10, and the carbapenem-resistant derivative R2091 was obtained. Genome sequencing of the R2091 derivative revealed that it had received an approximately 66-kb region comprising the transposon Tn*125* embedding the bla_{NDM-1} gene. This region had integrated into the chromosome of the recipient strain CIP 70.10. From the four known mechanisms for horizontal gene transfer (conjugation, outer membrane vesicle-mediated transfer, transformation, and transduction), conjugation could be ruled out, since strain R2090 lacks any plasmid, and a type IV secretion system is not encoded in its chromosome. However, strain R2090 possesses three putative prophages, two of which were predicted to be complete and therefore functional. Accordingly, it was supposed that the transfer of the resistance gene region from the clinical isolate R2090 to the recipient occurred by general transduction facilitated by one of the prophages present in the R2090 genome. Hence, phage-mediated transduction has to be taken into account for the dissemination of antibiotic resistance genes within the species *A. baumannii*.

Resistance of microorganisms to antimicrobial compounds poses a public health problem of growing importance. The development and dissemination of antibiotic resistance interfere with treatment regimens and increase costs in health care facilities (1). In particular, infections in immunocompromised patients may turn dramatically due to failure of antimicrobial therapy. *Acinetobacter* species are strictly aerobic, Gram-negative, coccobacillary rods (2). They were isolated from a variety of habitats, including soil, water, wastewater, and hospital environments (3, 4). Currently, the *Acinetobacter* genus comprises 52 species (http://www.bacterio.net/acinetobacter.html, http://www.ncbi.nlm.nih.gov/Taxonomy/), some of which are important human pathogens (5). *Acinetobacter baumannii* is the most prevalent species in clinical environments (4), whereas it occurs more rarely in natural habitats (6). *A. baumannii* usually is harmless for healthy persons, although some particular *A. baumannii* strains may cause severe infections in immunocompromised patients, which is a serious problem in intensive care units.

Compared to other Gram-negative pathogens, few virulence determinants have been identified in *A. baumannii* strains (6). Most *A. baumannii* virulence determinants belong to the core genome (7). However, a wide spectrum of resistance determinants and its high robustness make *A. baumannii* a serious nosocomial pathogen (8). It is able to rapidly acquire antibiotic resistance genes (9) by horizontal transfer from other bacteria, thus increasing its own virulence (10).

The multidrug-resistant *A. baumannii* strain R2090 was isolated from a hospitalized Egyptian patient. To analyze its putative and respective virulence and resistance determinants, the genome of *A. baumannii* R2090 was completely sequenced. A corresponding genome announcement was published recently (11). Here, pathogenicity and resistance determinants of the isolate were identified. Moreover, the relatedness of strain R2090 to other *A. baumannii* strains was analyzed to gain epidemiological insights, and the horizontal transmissibility of its bla_{NDM-1} carbapenemase gene was demonstrated.

MATERIALS AND METHODS

Isolation, cultivation, identification, and total DNA preparation of *A. baumannii* strains. *A. baumannii* strain R2090 was recovered from a rectal swab screening of a patient who was hospitalized in Egypt. *A. baumannii* strains R2090, CIP 70.10, and R2091 were cultured in Trypticase soy broth medium, and total DNA was extracted and purified using the QIAamp DNA minikit (Qiagen, Hombrechtikon, Switzerland). Identification of strain R2090 was performed by using the API 20NE system (bioMérieux, La Balme-les-Grottes, France). In addition, the sequence of

TABLE 1 Genome features of *A. baumannii* strains R2090, R2091, and CIP 70.10

Strain/plasmid	Size (bp)	G+C content (%)	Total no. of genes	No. of rRNA operons	No. of tRNAs	No. of CDSs	No. of genes with predicted function
R2090	3,819,158	39.04	3,694	6	73	3,603	2,615
R2091	3,939,746	38.97	3,705	6	71	3,616	2,632
pABR2091	7,742	37.56	13	0	0	13	3
CIP 70.10	3,928,513	38.92	3,695	6	71	3,606	2,630
pABCIP70.10	7,742	37.56	13	0	0	13	3

the strain's 16S rRNA gene was established and compared to database entries.

Resistance pattern assessment. Antibiotic susceptibility testing was evaluated and interpreted according to the guidelines of the Clinical and Laboratory Standards Institute (CLSI).

Transfer of the bla_{NDM-1} resistance gene region to the recipient strain *A. baumannii* CIP 70.10. Mating-out assays were performed using *A. baumannii* R2090 as a donor and *A. baumannii* CIP 70.10 as the recipient strain. After overnight (o/n) growth in Trypticase soy liquid medium, both strains were diluted (1:10), cultured for 1 h, and then mixed at a ratio of 1 to 4 (donor/recipient) in a total volume of 2 ml. Subsequently, this mixed culture was grown for 3 h at 37°C, and 200 μl of the culture was plated onto selective Mueller-Hinton agar medium supplemented with ticarcillin (100 μg/ml) and rifampin (100 μg/ml). Growing colonies were checked by PCR for the presence of the β-lactamase gene bla_{NDM-1} and also their resistance phenotypes (resistance to ticarcillin and carbapenems).

Sequencing and annotation of the *A. baumannii* R2090, CIP 70.10, and R2091 genomes. High-throughput sequencing on the Illumina MiSeq system and bioinformatic analyses of the obtained genome sequences were accomplished as previously described for *A. baumannii* R2090 and CIP 70.10 (11, 12). The genome sequence of *A. baumannii* R2091 was established by applying a strategy similar to that described for strains R2090 and CIP 70.10 (see above). An 8-kb mate-pair sequencing library was constructed for strain R2091 and sequenced on the Illumina MiSeq system. The assembly of obtained sequence reads was performed by using the GS *de novo* Assembler software (version 2.8; Roche). Genome sequences of all three strains (R2090, CIP 70.10, and R2091) were annotated within the GenDB annotation platform (13) based on the annotation of the reference strain *A. baumannii* AB307-0294 (GenBank accession no. CP001172) (14). Moreover, a COG annotation was performed by means of WebMGA, with an E value threshold of 1×10^{-20} (15). In addition, the genes discussed in this study were manually annotated, as published recently (16–18), applying pairwise BLASTx comparisons of encoded protein sequences.

Phylogenetic classification and multilocus sequence typing. Phylogenetic classification based on genome sequence information for the *A. baumannii* strains sequenced in this study was performed using EDGAR 2.0 (19). For calculation of a core-genome-based phylogenetic tree, the core genes of *A. baumannii* strains R2090 and CIP 70.10, as well as those of all sequenced *A. baumannii* reference strains available in the public EDGAR project EDGAR_*Acinetobacter*, were considered. Furthermore, a Web service (http://enve-omics.ce.gatech.edu/ani/) was used to calculate the average nucleotide identity (ANI) (20).

Moreover, the sequence types (ST) of *A. baumannii* strains R2090, CIP 70.10, and R2091 were determined using the *A. baumannii* multilocus sequence typing (MLST) database (http://pubmlst.org/perl/bigsdb/bigsdb.pl?db=pubmlst_abaumannii_pasteur_seqdef&page=sequenceQuery&set_id=2). The MLST is based on the allelic sequences of seven housekeeping genes (Pasteur scheme: *cpn*60, *fusA*, *gltA*, *pyrG*, *recA*, *rplB*, and *rpoB*) and was used for assignment to a clonal complex (CC), as defined previously (10, 21).

Detection of putative pathogenicity determinants and antibiotic resistance genes. Identification of the putative virulence factors and antibiotic resistance determinants in the genomes of the sequenced isolates was performed using the databases MvirDB (22), ARG-ANNOT (23), CARD (24), and Resfams (25). For the detection of determinants represented in the databases MvirDB and ARG-ANNOT, BLASTp (26) was applied, with an E value threshold of 1×10^{-100}. The CARD database was accessed using the Resistance Gene Identifier version 2 (http://arpcard.mcmaster.ca/). Furthermore, a hidden Markov model (HMM) search (27, 28) was performed, with an E value threshold of 1×10^{-100}, to identify putative resistance genes of the Resfams Core database. Moreover, the genomes were searched for relaxases and key components of type IV secretion systems using CONJscan-T4SSscan (http://mobyle.pasteur.fr/cgi-bin/portal.py#forms::CONJscan-T4SSscan) (29). Additionally, the PHAge Search Tool (PHAST) was used on the nucleic acid level for the prediction of integrated bacteriophages in the chromosomes (30).

Nucleotide sequence accession numbers. Genome sequences for *A. baumannii* strains R2090, CIP 70.10, and the CIP 70.10 derivative strain R2091 harboring the β-lactamase gene bla_{NDM-1} are accessible under the EMBL/GenBank accession no. LN868200 (R2090), LN865143 to LN865144 (CIP 70.10), and LN997846 to LN997847 (R2091).

RESULTS AND DISCUSSION

Origin of the clinical isolate *A. baumannii* R2090. Isolate R2090 was recovered during the course of hospital admission from a rectal swab from a colonized Egyptian patient who was transferred to a hospital in France. The obtained isolate showed resistance to all β-lactam antibiotics, including carbapenems at high levels (MICs for imipenem and meropenem, >32 μg/ml). The isolate was considered a colonizing strain, since the patient had not developed any infection symptoms related to *A. baumannii*.

Sequencing, general features, and phylogenetic analysis of the *A. baumannii* R2090 genome. Considering the multidrug resistance pattern of the isolated *A. baumannii* strain R2090, it was decided to sequence its genome to identify encoded antibiotic resistance and virulence determinants and to analyze its relatedness to known antibiotic-resistant *A. baumannii* reference strains, thereby addressing epidemiological aspects.

The genome sequence of the isolate *A. baumannii* R2090 was established by applying the Illumina MiSeq system, the GS *de novo* assembler (version 2.8; Roche), and the bioinformatics tool Consed (31), as described previously (11), combined with a PCR-based strategy leading to the amplification of a gap-spanning fragment that was sequenced to fill one remaining gap. Annotation of orthologous genes was performed within the annotation tool GenDB 2.4 (13) using the annotated genome sequence of *A. baumannii* strain AB307-0294 as a reference (14). The features of the R2090 chromosome sequence are depicted in Table 1 and Fig. 1.

Phylogenetic classification of *A. baumannii* R2090 was done within the comparative genomics tool EDGAR (19) based on *A. baumannii* core genes. The calculated phylogenetic tree (Fig. 2) involving 1,885 core genes of 18 *A. baumannii* strains features three main clusters and two outgroups. Clusters 1 and 2 represent clonal complexes CC1 and CC2 (10, 21), respectively, whereas the strains of cluster 3 and the two outgroup strains (SDF and CIP

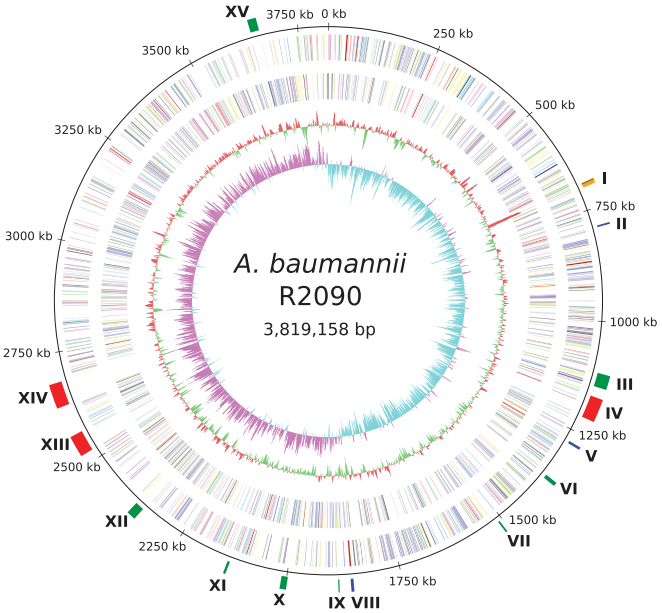

FIG 1 Circular representation of the *A. baumannii* R2090 chromosome. From the inside to the outside, the circles represent the GC skew (1), the G+C content (2), and the predicted protein-coding sequences (CDSs) on the reverse (3) and forward strand (4), colored according to the assigned Clusters of Orthologous Groups of proteins (COG) classes. Circle 5 displays the chromosome coordinates. In the sixth circle, regions described in the text are marked. These are related to predicted prophages (red), putative antibiotic resistance genes (blue), and virulence determinants (green), as well as the transposon Tn*125* (orange). I, transposon Tn*125* harboring bla_{NDM-1} gene; II, resistance-nodulation-division (RND) efflux pump AdeIJK; III, siderophore cluster (acinetobactin); IV, ΦR2090-I; V, RND efflux pump AdeFGH; VI, type I pilus cluster (Csu cluster); VII, type I pilus cluster (truncated); VIII, RND efflux pump AdeABC; IX, siderophore cluster; X, siderophore cluster; XI, type I pilus cluster (truncated); XII, type VI secretion system (truncated); XIII, ΦR2090-II; XIV, ΦR2090-III, XV, *N*-acyl homoserine lactone (AHL) cluster.

70.10) do not belong to clonal complex 1 or 2. The isolate *A. baumannii* R2090 shows the highest degree of relatedness to strain *A. baumannii* D1279779 (32). The high similarity of these two strains was also confirmed by average nucleotide identity (ANI) analysis, which resulted in an ANI of 99.92%. Strains R2090 and D1279779 both belong to the ST267, as determined by the Pasteur scheme via the corresponding Web tool PubMLST (21). The reference strain *A. baumannii* D1279779 originates from an indigenous Australian patient and represents the first fully sequenced community-acquired *A. baumannii* isolate (32).

Comparative analyses of the two closely related *A. baumannii* isolates R2090 and D1279779 regarding putative antibiotic resistance and virulence determinants. A chromosome-wide alignment of the two *A. baumannii* isolates R2090 and D1279779 applying progressiveMauve (33), visualized by Mauve (34) and GenomeRing (35), revealed an inversion of about 50 kb around the origin of replication in strain D1279779 in comparison to strain R2090 (Fig. 3). Moreover, structural differences in six regions >10 kb were detected (Fig. 3). Among these, two segments represent two of the three predicted prophage regions (described below). The four other regions comprised predicted mobile genetic elements (insertion sequence [IS] elements, other putative transposable elements, and a phage integrase gene). Regarding possible virulence factors and resistance determinants, two of these regions are of outstanding interest.

An approximately 20-kb region within the genome of strain R2090 is located in the vicinity of a transposase gene (ABR2090_2277). It harbored 13 genes of a putative type VI secretion system (T6SS) (ABR2090_2264 to ABR2090_2276) (36). Although a T6SS cluster was identified in most *A. baumannii* strains, it is not encoded in strain D1279779 (32, 37). Other conserved putative virulence genes of the species *A. baumannii* encoding a heme acquisition system (38) and the biofilm-associated protein Bap (39) were not identified in either strain R2090 or D1279779 (32). While the gene encoding the *Acinetobacter* trimeric autotransporter protein (Ata) (40) is truncated in strain D1279779 (32), the corresponding gene in strain R2090 carries a 627-bp insertion in comparison to the reference gene (A1S_1032) of *A. baumannii* strain ATCC 17978 (40, 41). Accordingly, Ata seems to be defective in both strains (37). As proposed by Farrugia et al. (32), the reduced biofilm formation activity of strain D1279779 is presumably due to the loss of the genes *ata* and *bap*, the T6SS cluster, and the heme acquisition system II. Strains

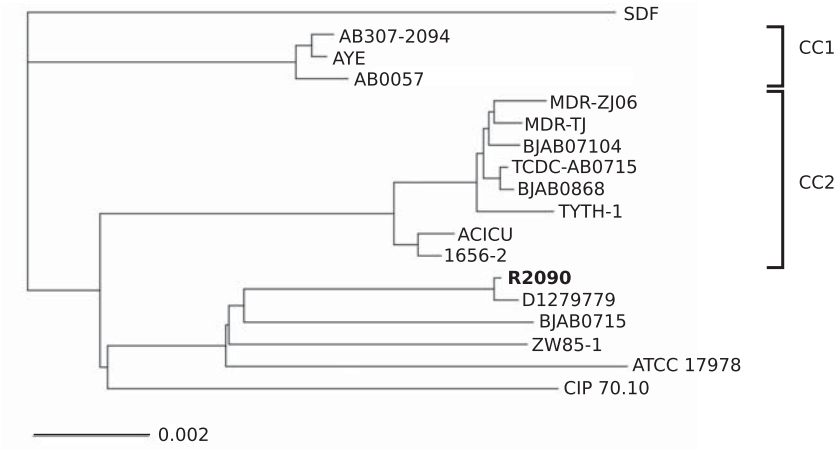

FIG 2 Phylogeny of different *A. baumannii* strains, as analyzed within the comparative genomics tool EDGAR based on core genes for all isolates. Phylogenetic analyses within EDGAR were essentially done as described previously (16, 19). Strains belonging to a specific clonal complex (CC) are labeled on the right-hand side. Strains SDF, R2090, D1279779, BJAB0715, ZW85-1, ATCC 17978, and CIP 70.10 belong to neither CC1 nor CC2.

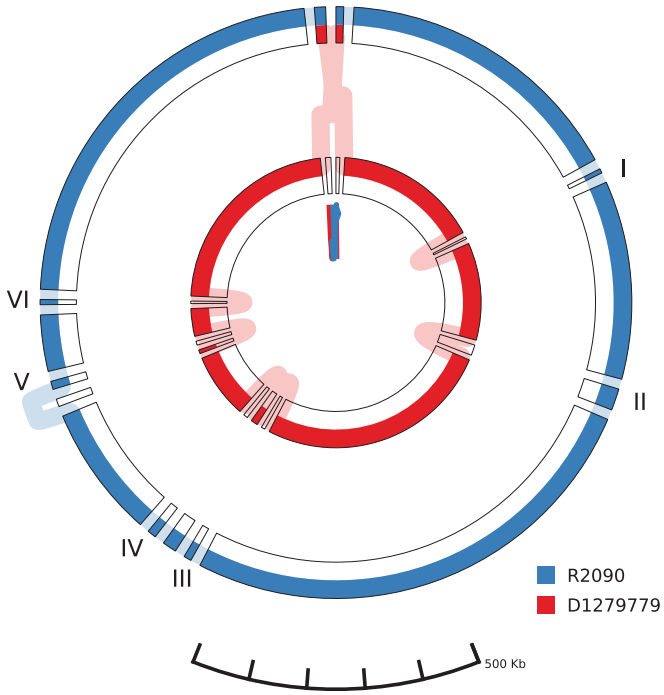

FIG 3 Comparison of the genomes of the *A. baumannii* isolates R2090 and D1279779. Visualization of the progressiveMauve (35) alignment with default settings of the chromosomes of strains R2090 and D1279799 was done by application of the visualization tool GenomeRing (37). Each chromosome is represented by a colored path (blue, *A. baumannii* R2090; red, *A. baumannii* D1279779). The chromosomes' start and end positions are labeled by triangles in the corresponding color. The outer and inner circles represent the forward and reverse orientations, respectively. All subblocks with a minimum block length of 10,000 bp are presented. Insertions in the R2090 chromosome are labeled and denote (I) the transposon Tn*125*, (II) prophage ΦR2090-I, (III) an ~17-kb region adjacent to the transposase gene ABR2090_2200, (IV) the truncated type VI secretion system cluster, (V) prophage ΦR2090-III, and (VI) an ~13-kb region adjacent to an integrase gene (ABR2090_2768). Prophage ΦR2090-II is not displayed in a separate block, as it possesses relatively high similarity to a prophage region in strain D1279779.

R2090 and D1279779 possess a similar gene layout concerning genes predicted to contribute to biofilm formation. However, no reliable prediction of biofilm formation capabilities can be given by these *in silico* analyses, since biofilm formation is a multifactor-regulated process. Moreover, R2090 possesses two truncated type I pilus gene clusters (ABR2090_1456 to ABR2090_1457 and ABR2090_2049to ABR2090_2050) (37) also specifying functions in biofilm formation. Further putative virulence factors predicted to be involved in iron acquisition, DNA uptake, and twitching motility do not show significant differences between the two strains (identities of corresponding gene products, ≥99.65%).

Another 11-kb region (Fig. 3 and 4) lacking in strain D1279779 is flanked by two insertion sequences of IS*Aba125* (ABR2090_0672 and ABR2090_0680) and carries the metallo-β-lactamase gene $bla_{\text{NDM-1}}$ (ABR2090_0673). This structure corresponds to the previously identified composite transposon Tn*125* (42, 43). Due to the presence of the carbapenemase gene $bla_{\text{NDM-1}}$, the isolate was indeed highly resistant to all β-lactams, including carbapenems. Since the $bla_{\text{NDM-1}}$ gene is located on a composite transposon, it was speculated that the whole element is mobile. To test the transmissibility of the predicted mobile element, strain R2090 was mated with another susceptible *A. baumannii* strain.

Transfer of the $bla_{\text{NDM-1}}$ resistance region from the clinical *A. baumannii* strain R2090 to the susceptible *A. baumannii* recipient strain CIP 70.10. The most important difference between the clinical *A. baumannii* strain R2090 and the closely related reference strain D1279779 is the integration of the metallo-β-lactamase resistance region $bla_{\text{NDM-1}}$ in R2090. A corresponding region is missing in strain D1279779. Since the $bla_{\text{NDM-1}}$ gene was located on the mobile genetic element Tn*125*, the question arose as to whether the element was acquired by horizontal gene transfer (HGT). To test the transmissibility of the $bla_{\text{NDM-1}}$ resistance region, a mating-out experiment between R2090 and the susceptible recipient strain *A. baumannii* CIP 70.10 was performed. Upon selection on agar medium supplemented with ticarcillin and rifampin, derivative strains arose with a frequency of $1/10^6$ (per recipient titer). PCR analyses and resistance testing confirmed that *A. baumannii* CIP 70.10 received the $bla_{\text{NDM-1}}$ gene and expressed the corresponding resistance pheno-

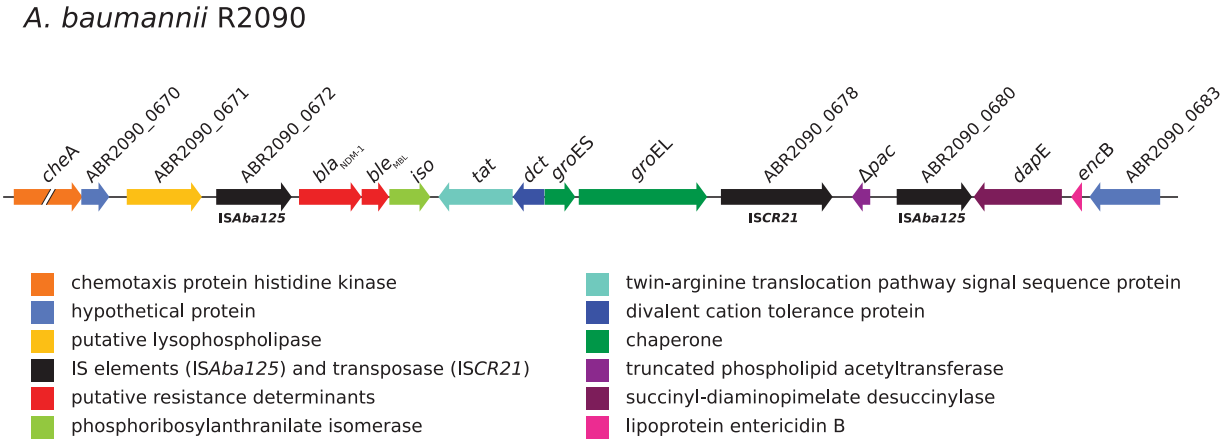

FIG 4 Schematic representation of transposon Tn*125* harboring the $bla_{\text{NDM-1}}$ gene. The *A. baumannii* R2090 chromosomal region (approximately 18.7 kb) harboring the transposon Tn*125* is located between coordinates 682069 and 700811. Coding sequences are labeled by either their gene name or locus tag. Lengths of coding sequences are drawn to scale, except for the chemotaxis gene *cheA*. Annotation of genes was adopted from previous publications (42, 56).

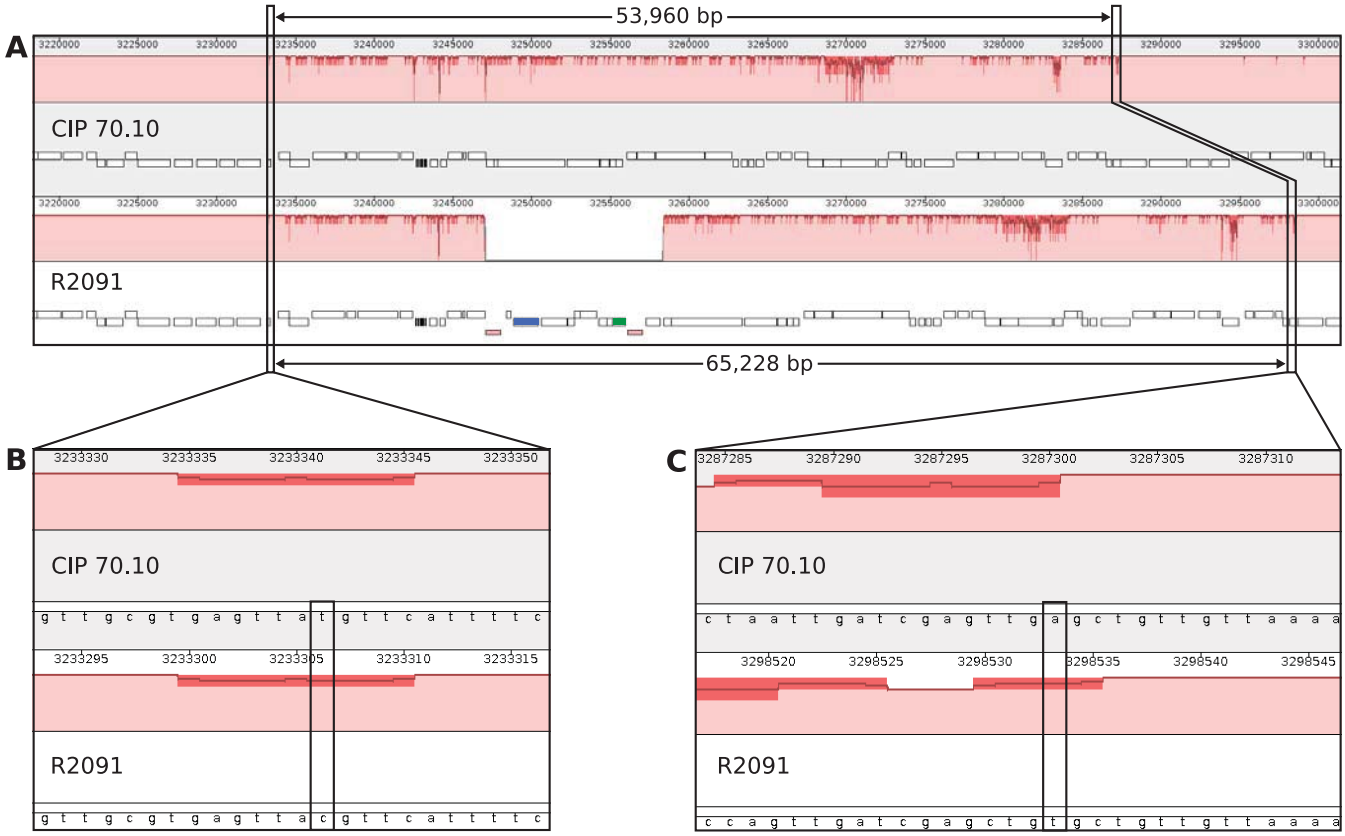

FIG 5 Pairwise alignment of the region carrying Tn*125* (bla_{NDM-1}) between the *A. baumannii* strain R2091 and the corresponding recipient strain CIP 70.10 obtained by using Mauve. Chromosome coordinates are plotted on the *x* axis, and the *y* axis denotes the percent sequence identity, with 100% representing completely identical sequences. (A) Chromosomal regions of strains CIP 70.10 and R2091 featuring comparatively low sequence similarity. Rectangles below the similarity plot represent coding sequences (CDSs). Colored rectangles denote the insertion sequence (IS) elements IS*Aba125* (red), a transposase gene (blue), and the gene bla_{NDM-1} (green). (B and C) Enlarged regions, in which possible homologous recombination events have occurred, are shown. First (B) and last (C) SNPs of the region featuring low sequence similarity are boxed. Beyond these SNPs, the chromosomal sequences of the strains are completely identical, except for very few minor mismatches presumably representing mutation events in one or the other genome or sequencing errors.

type (resistance to ticarcillin and carbapenems). One representative derivative clone, designated R2091, was chosen for further analysis to determine the extent of the transferred resistance gene region and its integration site in the host chromosome. For this purpose, the complete genome sequences of the derivative R2091 and the corresponding recipient strain CIP 70.10 were established.

Comparative genome sequence analyses of the derivative strain R2091 carrying the bla_{NDM-1} resistance region and the corresponding susceptible *A. baumannii* recipient strain CIP 70.10. The genome sequences of strain R2091 carrying the bla_{NDM-1} resistance gene and the corresponding susceptible recipient strain CIP 70.10 were established using the Illumina MiSeq system, essentially as described for the clinical *A. baumannii* isolate R2090 (see above). Sequencing statistics and genome features for the two strains are summarized in Table 1 (11, 12). In comparison to the genome of strain CIP 70.10, that of the derivative strain R2091 was 11,233 bp larger, which almost corresponds to the size of transposon Tn*125* carrying the bla_{NDM-1} gene. The G+C content of the R2091 genome was determined to be 38.97%, and it contained 3,616 coding sequences. The gene contents of strains CIP 70.10 and R2091 are nearly identical, except for 11 additional genes that are present only in the derivative R2091. These accessory genes were located on the transposon Tn*125* (see below).

To determine the chromosomal background of the derivative strain R2091 carrying the bla_{NDM-1} gene, multilocus sequence typing (MLST) and ANI analyses were carried out. The obtained results confirmed that R2091 features the chromosomal background of the recipient strain CIP 70.10. Both strains belong to sequence type 126 (ST126) and showed an ANI of 99.96%, whereas the clinical strain R2090 was assigned to ST267 and displayed an ANI of 97.73% to R2091. However, a chromosome-wide alignment by means of Mauve (34) of strains CIP 70.10 and R2091 (Fig. 5) revealed an approximately 65-kb region in R2091 (coordinates 3233306 to 3298533 bp) featuring a significantly lower ANI of 97.95% (Fig. 3). A large part of the 65-kb segment contains homologous genes, except for an 11-kb region (bp ~3247000 to 3287300) representing the described transposon Tn*125* harboring the bla_{NDM-1} gene. An alignment of the chromosomes of strains R2090 and R2091 confirmed that the 65 kb originates from the clinical strain R2090 (see Fig. S1 in the supplemental material). Precisely, a 66,182-bp region surrounding the transposon Tn*125* was identical between the R2090 and R2091 chromosomes, except for two single nucleotide polymorphisms (SNPs).

These analyses uncovered that a 66-kb region carrying the bla_{NDM-1} gene had been transferred from the clinical strain R2090

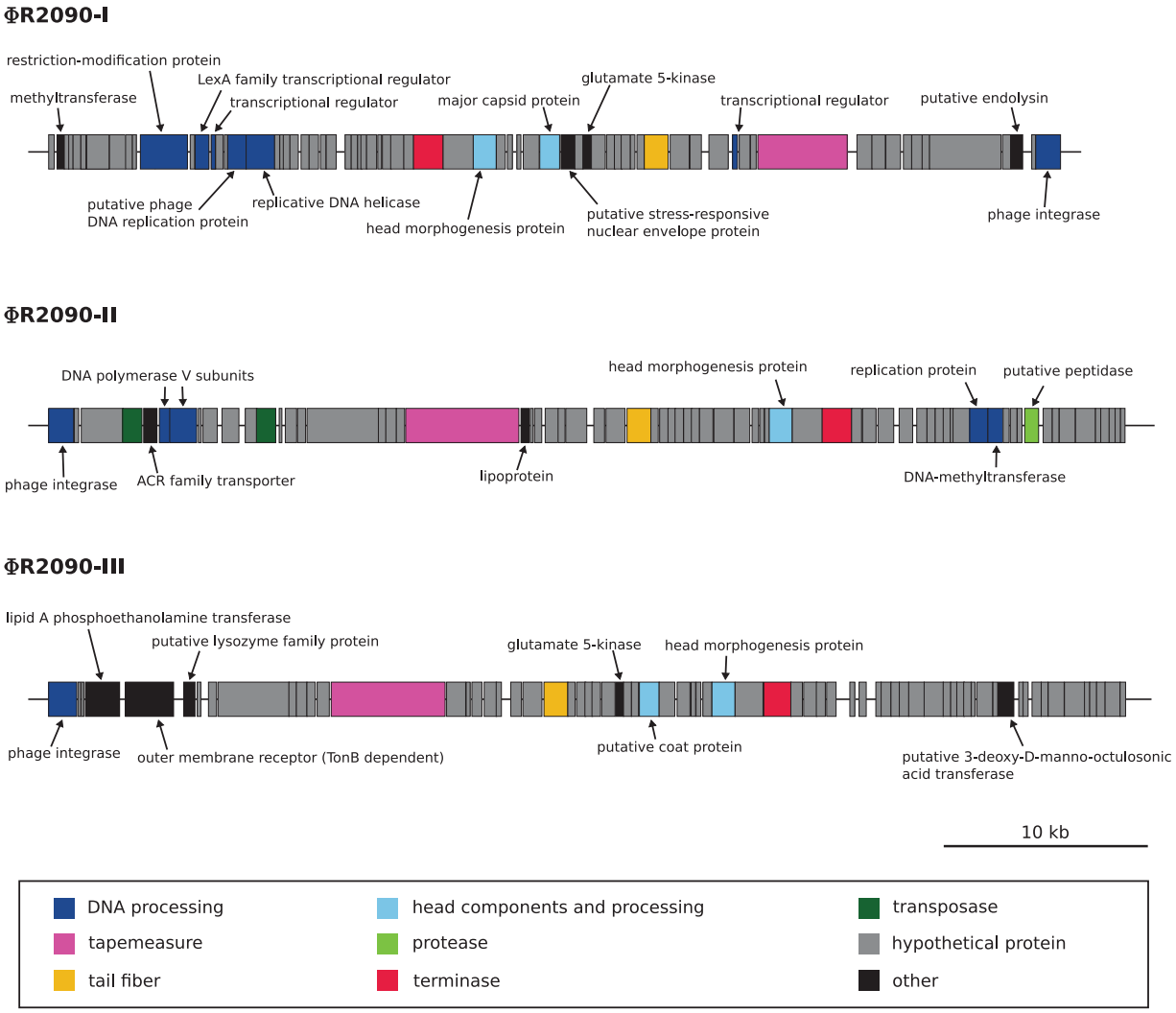

FIG 6 Predicted prophage regions within the *A. baumannii* R2090 chromosome. Putative prophage regions, as identified by application of the bioinformatics tool PHAST (30), each about 50 kb in size, are represented to scale. According to this analysis, ΦR2090-I (ABR2090_1106-1176) and ΦR2090-II (ABR2090_2421-2489) seem to be intact (scores, 91 and 110, respectively), whereas the completeness of ΦR2090-III (ABR2090_2555-2624) is not clear (score, 90). Phage-related genes are colored according to predicted functions of encoded gene products.

to the recipient strain CIP 70.10, in which it was integrated into the chromosome, presumably through homologous recombination. Four possible mechanisms have to be considered for the observed transfer of the resistance gene region from the donor to the recipient strain: (i) plasmid-mediated conjugative transfer, (ii) outer membrane vesicle (OMV)-mediated transfer, (iii) transformation, or (iv) phage-mediated transduction.

Plasmid-mediated transfer can be excluded, since strain R2090 lacks any plasmid. Moreover, a type IV secretion system (T4SS), required for mating-pair formation and conjugative DNA transfer to a recipient cell (44), is not encoded in the genome of isolate R2090, as determined by application of the bioinformatics tool CONJscan-T4SSscan (29). DNA transfer mediated by outer membrane vesicles (OMV) seems to be unlikely because of the size of the transferred region and its chromosomal location. Some *Acinetobacter* species are known to be able to transfer DNA via OMVs (45, 46). However, the transferred region in the case of strain R2090 seems to be too large for OMV-mediated transmission, since so far, only 10- to 25-kb fragments were observed to be transferred involving OMVs (45–47). Uptake of free DNA from the medium also is unlikely, although some *A. baumannii* strains previously were shown to be capable of natural transformation. *A. baumannii* CIP 70.10 encodes a type IV pilus (T4P) system and a channel formed by the proteins ComA/ComEC implicated in DNA uptake from outside the cell (48). However, transformation efficiency was shown to be very low for strain CIP 70.10 (49). Moreover, DNA uptake of fragments >50 kb by natural transformation currently has to be considered a great challenge for the cell (50), and nucleases may restrict incoming DNA (51).

Finally, larger DNA fragments can be transferred by phage-mediated general transduction. Application of the phage search tool PHAST (30) led to the prediction of two intact (from coordinates 1165468 to 1215544 and from 2514187 to 2568847) and one presumptive prophage region (from coordinates 2635367 to 2687628) in the R2090 genome (Fig. 6). The putative prophages show similarity to the reference phage BΦ-B1251 (YMC/09/02/

B1251 ABA BP) (52). Overall, 36 of the 62 CDSs of the reference phage were identified at least once in the R2090 chromosome, featuring identities of at least 90% at the amino acid sequence level. Manual analyses of the prophage regions revealed that they are each approximately 49 to 52 kb in size and comprise 69 to 71 CDSs (Fig. 6). The genes in the prophage regions are similar to those in other *A. baumannii* prophages, which were predicted to be intact (53). Genes known to be essential for phage activity, such as those specifying DNA processing, replication, structural components, morphogenesis, phage integration, and cell lysis, were identified (Fig. 6). Furthermore, the prophage regions ΦR2090-II and ΦR2090-III are bordered by putative attachment sites *attL* and *attR* (21 bp and 63 bp in size, respectively). Accordingly, prophage ΦR2090-II was predicted to be intact by means of the bioinformatics tool PHAST (score, 110), whereas ΦR2090-III was classified as questionable (score, 90), despite the predicted attachment sites. Although no valid attachment sites were identified for ΦR2090-I, it was categorized as intact by PHAST (score, 91). However, the activities of these phages remain to be confirmed.

It is thus conceivable that after phage-mediated lysis of R2090 donor cells, random DNA fragments were packaged into the capsid of the phage and subsequently transferred to the recipient cell via infection (transduction). Fragments of >100 kb were previously shown to be transferable by phage-mediated transduction (54). DNA introduced into a recipient cell by transduction can be integrated into the chromosome via RecA-dependent recombination (51) and thus may become manifested in the host's genome. Inspection of both ends of the transferred 66-kb fragment comprising the bla_{NDM-1} gene led to the identification of 180-bp and 774-bp flanking regions that are identical to corresponding regions present in the recipient chromosome of strain CIP 70.10. These sequences presumably are long enough to represent the target sites for homologous recombination (51, 55), leading to the integration of the resistance gene region into the chromosome of the recipient CIP 70.10.

Concluding remarks. The carbapenem-resistant *A. baumannii* strain R2090 originated from a colonized Egyptian patient who was admitted to a hospital in France. Interestingly, the isolated strain appeared to be closely related to *A. baumannii* strain D1279779 belonging to the ST267. The D1279779 reference strain was obtained from an indigenous Australian patient and represents a community-acquired isolate. The close relatedness of an Egyptian and Australian *A. baumannii* isolate again reflects the dissemination of opportunistic pathogenic bacteria due to long-distance travel opportunities, and it sheds light on *A. baumannii* epidemiology. The main difference between strains R2090 and D1279779 is that the isolate R2090 harbors a gene encoding the New Delhi metallo-β-lactamase NDM-1, which mediates carbapenem resistance. The presence of this gene severely complicates the treatment of *A. baumannii* infections by application of β-lactam antibiotics. Basically, it was not possible to deduce how the bla_{NDM-1} gene was acquired by strain R2090, since it is not located on a mobile plasmid but appeared to be integrated in the host's chromosome. However, the β-lactamase resistance gene is flanked by two different insertion sequence elements (IS*Aba125* and IS*CR21*) that potentially enable movement (translocation) of the bla_{NDM-1} gene. It has been shown experimentally that the resistance gene region could be transferred from the strain R2090 to a susceptible *A. baumannii* recipient strain. Commonly, mobile plasmids are involved in the horizontal transfer of resistance determinants between bacteria. However, since strain R2090 does not contain any plasmid, another mechanism must account for the resistance gene transfer observed. Natural transformation, outer membrane vesicle-mediated transfer, or transduction facilitated by phages have to be considered for horizontal gene transfer. The first two mechanisms were previously shown to enable the transfer of relatively short DNA fragments. In the case of strain R2090, an approximately 66-kb fragment was transferred to the *A. baumannii* recipient strain CIP 70.10. Since isolate R2090 possesses three presumably intact prophages integrated in its chromosome, it is very likely that activation of one of these prophages may have facilitated transduction of the bla_{NDM-1} gene. Although general transduction accomplished by phages is not as efficient as conjugative plasmid-mediated gene transfer, it has to be taken into account for the dissemination of resistance genes among *Acinetobacter* strains. Hence, phages may contribute to the adaptation of pathogenic *Acinetobacter* species to selective pressure caused by the presence of antibiotics.

ACKNOWLEDGMENTS

The bioinformatics support of the BMBF-funded project Bielefeld-Giessen Center for Microbial Bioinformatics (BiGi) (grant 031A533) within the German Network for Bioinformatics Infrastructure (de.NBI) is gratefully acknowledged. I. Maus and D. Wibberg acknowledge the receipt of a scholarship from the CLIB Graduate Cluster Industrial Biotechnology, cofinanced by the Ministry of Innovation of North Rhine-Westphalia, Germany. This work has also been financed by the University of Fribourg, Switzerland, and by the Swiss National Fund (SNF) under grant 31003A_163432/1.

FUNDING INFORMATION

This work, including the efforts of Alfred Pühler, was funded by German Federal Ministry of Education and Research (031A533). This work, including the efforts of Daniel Wibberg and Irena Maus, was funded by Ministry of Innovation of North Rhine-Westphalia, Germany. This work, including the efforts of Patrice Nordmann and Laurent Poirel, was funded by Swiss National Fund, SNF (31003A_163432/1).

REFERENCES

1. **Levy SB, Marshall B.** 2004. Antibacterial resistance worldwide: causes, challenges and responses. Nat Med **10:**122–129. http://dx.doi.org/10.1038/nm0204-122.
2. **Vallenet D, Nordmann P, Barbe V, Poirel L, Mangenot S, Bataille E, Dossat C, Gas S, Kreimeyer A, Lenoble P, Oztas S, Poulain J, Segurens B, Robert C, Abergel C, Claverie J-M, Raoult D, Médigue C, Weissenbach J, Cruveiller S.** 2008. Comparative analysis of *Acinetobacters*: three genomes for three lifestyles. PLoS One **3:**e1805. http://dx.doi.org/10.1371/journal.pone.0001805.
3. **Juni E.** 1978. Genetics and physiology of *Acinetobacter*. Annu Rev Microbiol **32:**349–371. http://dx.doi.org/10.1146/annurev.mi.32.100178.002025.
4. **Cerqueira GM, Peleg AY.** 2011. Insights into *Acinetobacter baumannii* pathogenicity. IUBMB Life **63:**1055–1060. http://dx.doi.org/10.1002/iub.533.
5. **Bouvet PJM, Grimont PAD.** 1986. Taxonomy of the genus *Acinetobacter* with the recognition of *Acinetobacter baumannii* sp. nov., *Acinetobacter haemolyticus* sp. nov., *Acinetobacter johnsonii* sp. nov., and *Acinetobacter junii* sp. nov. and emended descriptions *Acinetobacter calcoaceticus* and *Acinetobacter lwoffii*. Int J Syst Bacteriol **36:**228–240. http://dx.doi.org/10.1099/00207713-36-2-228.
6. **Dijkshoorn L, Nemec A, Seifert H.** 2007. An increasing threat in hospitals: multidrug-resistant *Acinetobacter baumannii*. Nat Rev Microbiol **5:**939–951. http://dx.doi.org/10.1038/nrmicro1789.
7. **Touchon M, Cury J, Yoon E-J, Krizova L, Cerqueira GC, Murphy C, Feldgarden M, Wortman J, Clermont D, Lambert T, Grillot-Courvalin C, Nemec A, Courvalin P, Rocha EPC.** 2014. The genomic diversification

of the whole *Acinetobacter* genus: origins, mechanisms, and consequences. Genome Biol Evol **6:**2866–2882. http://dx.doi.org/10.1093/gbe/evu225.

8. **Perez F, Hujer AM, Hujer KM, Decker BK, Rather PN, Bonomo RA.** 2007. Global challenge of multidrug-resistant *Acinetobacter baumannii*. Antimicrob Agents Chemother **51:**3471–3484. http://dx.doi.org/10.1128/AAC.01464-06.
9. **Fournier P-E, Vallenet D, Barbe V, Audic S, Ogata H, Poirel L, Richet H, Robert C, Mangenot S, Abergel C, Nordmann P, Weissenbach J, Raoult D, Claverie J-M.** 2006. Comparative genomics of multidrug resistance in *Acinetobacter baumannii*. PLoS Genet **2:**e7. http://dx.doi.org/10.1371/journal.pgen.0020007.
10. **Imperi F, Antunes LCS, Blom J, Villa L, Iacono M, Visca P, Carattoli A.** 2011. The genomics of *Acinetobacter baumannii*: insights into genome plasticity, antimicrobial resistance and pathogenicity. IUBMB Life **63:**1068–1074. http://dx.doi.org/10.1002/iub.531.
11. **Krahn T, Wibberg D, Maus I, Winkler A, Nordmann P, Pühler A, Poirel L, Schlüter A.** 2015. Complete genome sequence of the clinical strain *Acinetobacter baumannii* R2090 carrying the chromosomally encoded metallo-β-lactamase gene bla_{NDM-1}. Genome Announc **3**(5):e01008-15. http://dx.doi.org/10.1128/genomeA.01008-15.
12. **Krahn T, Wibberg D, Maus I, Winkler A, Pühler A, Poirel L, Schlüter A.** 2015. Complete genome sequence of *Acinetobacter baumannii* CIP 70.10, a susceptible reference strain for comparative genome analyses. Genome Announc **3**(4)**:**e00850-15. http://dx.doi.org/10.1128/genomeA.00850-15.
13. **Meyer F, Goesmann A, McHardy AC, Bartels D, Bekel T, Clausen J, Kalinowski J, Linke B, Rupp O, Giegerich R, Pühler A.** 2003. GenDB: an open source genome annotation system for prokaryote genomes. Nucleic Acids Res **31:**2187–2195. http://dx.doi.org/10.1093/nar/gkg312.
14. **Adams MD, Goglin K, Molyneaux N, Hujer KM, Lavender H, Jamison JJ, MacDonald IJ, Martin KM, Russo T, Campagnari AA, Hujer AM, Bonomo RA, Gill SR.** 2008. Comparative genome sequence analysis of multidrug-resistant *Acinetobacter baumannii*. J Bacteriol **190:**8053–8064. http://dx.doi.org/10.1128/JB.00834-08.
15. **Wu S, Zhu Z, Fu L, Niu B, Li W.** 2011. WebMGA: a customizable Web server for fast metagenomic sequence analysis. BMC Genomics **12:**444. http://dx.doi.org/10.1186/1471-2164-12-444.
16. **Wibberg D, Blom J, Jaenicke S, Kollin F, Rupp O, Scharf B, Schneiker-Bekel S, Szczepanowski R, Goesmann A, Setubal JC, Schmitt R, Pühler A, Schlüter A.** 2011. Complete genome sequencing of *Agrobacterium* sp. H13-3, the former *Rhizobium lupini* H13-3, reveals a tripartite genome consisting of a circular and a linear chromosome and an accessory plasmid but lacking a tumor-inducing Ti-plasmid. J Biotechnol **155:**50–62.
17. **Heinl S, Wibberg D, Eikmeyer F, Szczepanowski R, Blom J, Linke B, Goesmann A, Grabherr R, Schwab H, Pühler A, Schlüter A.** 2012. Insights into the completely annotated genome of *Lactobacillus buchneri* CD034, a strain isolated from stable grass silage. J Biotechnol **161:**153–166. http://dx.doi.org/10.1016/j.jbiotec.2012.03.007.
18. **Eikmeyer F, Hadiati A, Szczepanowski R, Wibberg D, Schneiker-Bekel S, Rogers LM, Brown CJ, Top EM, Pühler A, Schlüter A.** 2012. The complete genome sequences of four new IncN plasmids from wastewater treatment plant effluent provide new insights into IncN plasmid diversity and evolution. Plasmid **68:**13–24. http://dx.doi.org/10.1016/j.plasmid.2012.01.011.
19. **Blom J, Albaum SP, Doppmeier D, Pühler A, Vorhölter F-J, Zakrzewski M, Goesmann A.** 2009. EDGAR: a software framework for the comparative analysis of prokaryotic genomes. BMC Bioinformatics **10:**154. http://dx.doi.org/10.1186/1471-2105-10-154.
20. **Konstantinidis KT, Ramette A, Tiedje JM.** 2006. The bacterial species definition in the genomic era. Philos Trans R Soc Lond B Biol Sci **361:**1929–1940. http://dx.doi.org/10.1098/rstb.2006.1920.
21. **Diancourt L, Passet V, Nemec A, Dijkshoorn L, Brisse S.** 2010. The population structure of *Acinetobacter baumannii*: expanding multiresistant clones from an ancestral susceptible genetic pool. PLoS One **5:**e10034. http://dx.doi.org/10.1371/journal.pone.0010034.
22. **Zhou CE, Smith J, Lam M, Zemla A, Dyer MD, Slezak T.** 2007. MvirDB: a microbial database of protein toxins, virulence factors and antibiotic resistance genes for bio-defence applications. Nucleic Acids Res **35:**D391–D394. http://dx.doi.org/10.1093/nar/gkl791.
23. **Gupta SK, Padmanabhan BR, Diene SM, Lopez-Rojas R, Kempf M, Landraud L, Rolain J-M.** 2014. ARG-ANNOT, a new bioinformatic tool to discover antibiotic resistance genes in bacterial genomes. Antimicrob Agents Chemother **58:**212–220. http://dx.doi.org/10.1128/AAC.01310-13.
24. **McArthur AG, Waglechner N, Nizam F, Yan A, Azad MA, Baylay AJ, Bhullar K, Canova MJ, De Pascale G, Ejim L, Kalan L, King AM, Koteva K, Morar M, Mulvey MR, O'Brien JS, Pawlowski AC, Piddock LJV, Spanogiannopoulos P, Sutherland AD, Tang I, Taylor PL, Thaker M, Wang W, Yan M, Yu T, Wright GD.** 2013. The Comprehensive Antibiotic Resistance Database. Antimicrob Agents Chemother **57:**3348–3357. http://dx.doi.org/10.1128/AAC.00419-13.
25. **Gibson MK, Forsberg KJ, Dantas G.** 2015. Improved annotation of antibiotic resistance determinants reveals microbial resistomes cluster by ecology. ISME J **9:**207–216. http://dx.doi.org/10.1038/ismej.2014.106.
26. **Altschul SF, Gish W, Miller W, Myers EW, Lipman DJ.** 1990. Basic Local Alignment Search Tool. J Mol Biol **215:**403–410. http://dx.doi.org/10.1016/S0022-2836(05)80360-2.
27. **Eddy SR.** 2009. A new generation of homology search tools based on probabilistic inference. Genome Inform **23:**205–211.
28. **Eddy SR.** 2011. Accelerated profile HMM searches. PLoS Comput Biol **7:**e1002195. http://dx.doi.org/10.1371/journal.pcbi.1002195.
29. **Guglielmini J, Quintais L, Garcillán-Barcia MP, de la Cruz F, Rocha EPC.** 2011. The repertoire of ICE in prokaryotes underscores the unity, diversity, and ubiquity of conjugation. PLoS Genet **7:**e1002222. http://dx.doi.org/10.1371/journal.pgen.1002222.
30. **Zhou Y, Liang Y, Lynch KH, Dennis JJ, Wishart DS.** 2011. PHAST: a fast phage search tool. Nucleic Acids Res **39:**W347–W352. http://dx.doi.org/10.1093/nar/gkr485.
31. **Gordon D, Abajian C, Green P.** 1998. Consed: a graphical tool for sequence finishing. Genome Res **8:**195–202. http://dx.doi.org/10.1101/gr.8.3.195.
32. **Farrugia DN, Elbourne LDH, Hassan KA, Eijkelkamp BA, Tetu SG, Brown MH, Shah BS, Peleg AY, Mabbutt BC, Paulsen IT.** 2013. The complete genome and phenome of a community-acquired *Acinetobacter baumannii*. PLoS One **8:**e58628. http://dx.doi.org/10.1371/journal.pone.0058628.
33. **Darling AE, Mau B, Perna NT.** 2010. progressiveMauve: multiple genome alignment with gene gain, loss and rearrangement. PLoS One **5:**e11147. http://dx.doi.org/10.1371/journal.pone.0011147.
34. **Darling ACE, Mau B, Blattner FR, Perna NT.** 2004. Mauve: multiple alignment of conserved genomic sequence with rearrangements. Genome Res **14:**1394–1403. http://dx.doi.org/10.1101/gr.2289704.
35. **Herbig A, Jäger G, Battke F, Nieselt K.** 2012. GenomeRing: alignment visualization based on SuperGenome coordinates. Bioinformatics **28:**i7–i15. http://dx.doi.org/10.1093/bioinformatics/bts217.
36. **Bingle LE, Bailey CM, Pallen MJ.** 2008. Type VI secretion: a beginner's guide. Curr Opin Microbiol **11:**3–8. http://dx.doi.org/10.1016/j.mib.2008.01.006.
37. **Eijkelkamp BA, Stroeher UH, Hassan KA, Paulsen IT, Brown MH.** 2014. Comparative analysis of surface-exposed virulence factors of *Acinetobacter baumannii*. BMC Genomics **15:**1020. http://dx.doi.org/10.1186/1471-2164-15-1020.
38. **Wilks A, Burkhard KA.** 2007. Heme and virulence: how bacterial pathogens regulate, transport and utilize heme. Nat Prod Rep **24:**511–522. http://dx.doi.org/10.1039/b604193k.
39. **Loehfelm TW, Luke NR, Campagnari AA.** 2008. Identification and characterization of an *Acinetobacter baumannii* biofilm-associated protein. J Bacteriol **190:**1036–1044. http://dx.doi.org/10.1128/JB.01416-07.
40. **Bentancor LV, Camacho-Peiro A, Bozkurt-Guzel C, Pier GB, Maira-Litrán T.** 2012. Identification of Ata, a multifunctional trimeric autotransporter of *Acinetobacter baumannii*. J Bacteriol **194:**3950–3960. http://dx.doi.org/10.1128/JB.06769-11.
41. **Smith MG, Gianoulis TA, Pukatzki S, Mekalanos JJ, Ornston LN, Gerstein M, Snyder M.** 2007. New insights into *Acinetobacter baumannii* pathogenesis revealed by high-density pyrosequencing and transposon mutagenesis. Genes Dev **21:**601–614. http://dx.doi.org/10.1101/gad.1510307.
42. **Bonnin RA, Poirel L, Naas T, Pirs M, Seme K, Schrenzel J, Nordmann P.** 2012. Dissemination of New Delhi metallo-β-lactamase-1-producing *Acinetobacter baumannii* in Europe. Clin Microbiol Infect **18:**E362–E365. http://dx.doi.org/10.1111/j.1469-0691.2012.03928.x.
43. **Pfeifer Y, Wilharm G, Zander E, Wichelhaus TA, Göttig S, Hunfeld K-P, Seifert H, Witte W, Higgins PG.** 2011. Molecular characterization of bla_{NDM-1} in an *Acinetobacter baumannii* strain isolated in Germany in

2007. J Antimicrob Chemother **66:**1998–2001. http://dx.doi.org/10.1093/jac/dkr256.

44. **de la Cruz F, Frost LS, Meyer RJ, Zechner EL.** 2010. Conjugative DNA metabolism in Gram-negative bacteria. FEMS Microbiol Rev **34:**18–40. http://dx.doi.org/10.1111/j.1574-6976.2009.00195.x.
45. **Rumbo C, Fernández-Moreira E, Merino M, Poza M, Mendez JA, Soares NC, Mosquera A, Chaves F, Bou G.** 2011. Horizontal transfer of the OXA-24 carbapenemase gene via outer membrane vesicles: a new mechanism of dissemination of carbapenem resistance genes in *Acinetobacter baumannii*. Antimicrob Agents Chemother **55:**3084–3090. http://dx.doi.org/10.1128/AAC.00929-10.
46. **Dallo SF, Zhang B, Denno J, Hong S, Tsai A, Haskins W, Ye JY, Weitao T.** 2012. Association of *Acinetobacter baumannii* EF-Tu with cell surface, outer membrane vesicles, and fibronectin. ScientificWorldJournal **2012:**128705.
47. **Yaron S, Kolling GL, Simon L, Matthews KR.** 2000. Vesicle-mediated transfer of virulence genes from *Escherichia coli* O157:H7 to other enteric bacteria. Appl Environ Microbiol **66:**4414–4420. http://dx.doi.org/10.1128/AEM.66.10.4414-4420.2000.
48. **Wilharm G, Piesker J, Laue M, Skiebe E.** 2013. DNA uptake by the nosocomial pathogen *Acinetobacter baumannii* occurs during movement along wet surfaces. J Bacteriol **195:**4146–4153. http://dx.doi.org/10.1128/JB.00754-13.
49. **Marchand I, Damier-Piolle L, Courvalin P, Lambert T.** 2004. Expression of the RND-type efflux pump AdeABC in *Acinetobacter baumannii* is regulated by the AdeRS two-component system. Antimicrob Agents Chemother **48:**3298–3304. http://dx.doi.org/10.1128/AAC.48.9.3298-3304.2004.
50. **Mell JC, Redfield RJ.** 2014. Natural competence and the evolution of DNA uptake specificity. J Bacteriol **196:**1471–1483. http://dx.doi.org/10.1128/JB.01293-13.
51. **Palmen R, Hellingwerf KJ.** 1997. Uptake and processing of DNA by *Acinetobacter calcoaceticus*: a review. Gene **192:**179–190. http://dx.doi.org/10.1016/S0378-1119(97)00042-5.
52. **Jeon J, Kim J, Yong D, Lee K, Chong Y.** 2012. Complete genome sequence of the podoviral bacteriophage YMC/09/02/B1251 ABA BP, which causes the lysis of an OXA-23-producing carbapenem-resistant *Acinetobacter baumannii* isolate from a septic patient. J Virol **86:**12437–12438. http://dx.doi.org/10.1128/JVI.02132-12.
53. **Hare JM, Ferrell JC, Witkowski TA, Grice AN.** 2014. Prophage induction and differential RecA and UmuDAb transcriptome regulation in the DNA damage responses of *Acinetobacter baumannii* and *Acinetobacter baylyi*. PLoS One **9:**e93861. http://dx.doi.org/10.1371/journal.pone.0093861.
54. **Ochman H, Lawrence JG, Groisman EA.** 2000. Lateral gene transfer and the nature of bacterial innovation. Nature **405:**299–304. http://dx.doi.org/10.1038/35012500.
55. **Nelson RT, Pryor BA, Lodge JK.** 2003. Sequence length required for homologous recombination in *Cryptococcus neoformans*. Fungal Genet Biol **38:**1–9. http://dx.doi.org/10.1016/S1087-1845(02)00510-8.
56. **Bonnin RA, Poirel L, Nordmann P.** 2014. New Delhi metallo-β-lactamase-producing *Acinetobacter baumannii*: a novel paradigm for spreading antibiotic resistance genes. Future Microbiol **9:**33–41. http://dx.doi.org/10.2217/fmb.13.69.